INFLUENȚA ELECTROZILOR ȘI A CONDIȚIILOR DE TESTARE ÎN DETERMINAREA REZISTENȚEI ȘI PIEZOREZISTENȚEI PASTEI DE CIMENT CU NANOFIBRE DE CARBON

INFLUENCE OF ELECTRODES AND TESTING CONDITIONS ON RESISTANCE AND PIEZORESISTIVITY OF CARBON NANOFIBERS CEMENT PASTE

HUI WANG[1] , XIAOJIAN GAO[1,2]*, ANASTASIIA GARIPOVA[1], HUALONG YANG[1]

[1] *School of Civil Engineering, Harbin Institute of Technology, Harbin 150090, China*

[2] *Key Lab of Structure Dynamic Behavior and Control (Harbin Institute of Technology), Ministry of Education, Harbin 150090, China*

This paper investigated the influence of embedded electrode and pasted electrode on the resistivity behavior of carbon nanofibers (CNFs) cement paste by using the alternating current (AC) method. The dosage of CNFs ranged from 0.75% to 3.125 % by volume of cement and the samples were measured after four treatment conditions including oven dried for 3 days, being sealed for 30 days, immersed in tap water or 3.5% NaCl solution for 30 days respectively. The piezoresistive performances of carbon nanofibers cement pastes (CNFP) with two types of electrodes under oven dry state were also studied. Results indicated that the average value and variability coefficient (C_v) of electrical resistivity were reduced by the increase of AC frequency only if the CNFs content was less than 2.5 vol.%. The immersion of water and NaCl solution reduced the resistivity of CNFP when the CNFs dosage is below 2.5 vol.%. The CNFP with pasted electrodes presented higher resistivity than the specimen with embedded electrodes when the CNFs content was lower than 3.125 vol.%. However, as the CNF content exceeded 2.5vol.%, the resistivity of CNFP with two types of electrodes were almost the same. The CNFP with two electrode types presented different piezoresistive performances at various amount of CNFs. A computational model for the piezoresistivity of CNFs cement paste was obtained from this research. The results of this research also demonstrated the improving effects of CNFs on the ductility and axial compressive strength of CNFP.

Keywords: *Carbon nanofibers; Cement paste; Electrode types; AC Frequency; Saturation degree; Resistivity; Piezoresistivity; Compressive strength*

1. Introduction

In recent years, structural health monitoring plays an important role in the research of the damage accumulation and disaster evolving characteristics of civil infrastructures. Reasonable monitoring methods can ensure the health and safety of civil infrastructures [1-3]. It is significant to monitor stress, strain and crack of the concrete structures for mitigating hazard in civil engineering field [4, 5]. The electric-resistance strain gauges, optic sensors, piezoelectric ceramic, shape memory alloy have been used in health monitoring for several years [6-10]. However, most of electric-resistance strain gauges show low sensitivity and reliability and optic sensors need complex embedding technology. Moreover, optic sensors achieve low survival embedding ratio and expensive demodulation [11-13].

Concrete incorporating some functional fillers like carbon fibers [14], carbon nanotubes [15], carbon blacks [16], carbon nanofibers (CNFs) [17] can be used to sense the strain, stress, crack or damage by itself. This self-monitoring method has high sensitivity, low cost and simple construction procedure. However, the design of electrode for self - sensing concrete is the key problem and the testing method and environment will affect the signal accuracy and basic configuration of sensors [18]. CNF is an elegant engineered material with hollow cylinder diameter around 100nm and length of a few microns. CNFs are presented by numerous exposed edge planes along the surface, which in turn constitute potential advantages of chemical or physical interaction in comparison with carbon nanotube (CNT). The CNFs can be manufactured in about 3~10 times cheaper than carbon nanotube [19].

Measuring the electrical resistance of intrinsic sensing concrete with the direct current (DC) test has been studied by many researchers for many years [1, 2, 7, 8]. The DC method leads to a notable electrical polarization which is dominated by ionic conduction resulting in the instability of the resistance test. The electrical polarization can be lessened to an acceptable range by an alternating current (AC) signals with equal magnitudes of positive and negative peaks to the composite [20]. However, few researches focused on the study of the influence of conditional testing conditions on the resistance of CNFP, including: specimen dry or wet state, CNFs content and electrode installation methods (embedded or pasted).

* Autor corespondent/*Corresponding author*,
E-mail: gaoxj@hit.edu.cn

In this paper the influence of electrode types on the resistivity of CNFP was determined at the AC frequency of 100Hz, 1000Hz and 10 kHz after drying for 72h. The resistivities of CNFP with two types of electrodes were also tested after being saturated in the water or 3.5% NaCl solution for 30 days under the AC frequency of 10 kHz. The piezoresistivities were studied for CNFP with two types of electrodes after drying for 72h. The optimum testing frequency and the advantages and limitations of the embedded electrode and pasted electrode were obtained from this study. Finally, based on experimental research of CNFP, a suitable piezoresistive computational model for CNFs cement paste was obtained.

2. Experimental

2.1. Raw materials

Carbon nanofiber used in this study is made by Pyrograf Products, Inc. The fiber is PR-19-XT-LHT-OX fiber, with a density of 2.1 g/cm^3. The diameter of this fiber was 149 nm and the length was 19μm resulting in an aspect ratio of 128. The cement used was ordinary Portland cement with strength grade of 42.5 according to Chinese standard GB175-2007 [21]. A commercially available, polycarboxylate-based, high-range water-reducing agent (SP) was used to adjust the flowability of the fresh cement paste. A defoamer, tributyl phosphate (made in China), was used in the amount of 0.2% by mass of cement to decrease the content of air bubbles.

2.2. Mixing proportion and specimen preparation

The water to cement ratio was kept as 0.4, the dosage of CNFs was increased from 0% to 3.125 % by volume of the cement. C0, C075, C125, C150, C175, C200, C250 and C3125 represented CNFP specimens containing CNFs dosages of 0%, 0.75%, 1.25%, 1.50%, 1.75%. 2.0%, 2.5% and 3.125% respectively. Suitable dosage of SP was adjusted for controlling the slump flow of the paste to around 200 mm.

Firstly, the water-reducing agent, CNFs, the defoamer and water were mixed in an ultrasonic cleaning machine for 3 hours then in a cement mixer for about 4 min. Afterwards the cement was added and stirred in the mixer for another 4 min. Ready mixture was poured into oiled moulds and was vibrated to remove air bubbles. For each mixture, 8 specimens with size of 20×20×25 mm were prepared and demoulded after 1 day curing at room temperature. For accelerating the experiment, the specimens were cured for another 3 days under temperature of 80±2℃ and relative humidity of higher than 95%. Then, the specimens were divided into four groups for different treatments including oven dried for 3 days, being sealed for 30 days, immersed in tap water or 3.5% NaCl solution for 30 days respectively.

The resistance was measured by an AC resistance measurement TH2810D LCR digital electric bridge produced by Changzhou Tonghui electronics co., LTD. The specimens were dried at 60℃ for 72h to reduce the polarization effect before the electrical resistivity measurement.

Pasted electrode means that two pieces of polyester conductive adhesive tape are pasted by silver paint on the two parallel planes of specimens, whereas the embedded electrode means the embedment of poles into the net of specimens with two corrosion resistant 304 stainless steels, as shown in Figure 1.

The electrical resistivity ρ can be calculated by the following equation [22].

$$\rho = RS / L \tag{1}$$

Where S is the effective area of voltage pole, L is the space between two electrodes and R is the volume resistance of the cement paste specimen.

The mean value and variable coefficient of the resistivity in each group were used to evaluate the stability of CNFP with two kinds of electrodes. The variability coefficient C_v was calculated by the following equation.

$$C_v = \frac{\sqrt{\sum_{i=1}^{n} (\rho_i - \bar{\rho})^2 / (n-1)}}{\bar{\rho}} \tag{2}$$

Where ρ_i (i=1~8) is the resistivity for specimen i_{th}, $\bar{\rho}$ is the average resistivity value of 8 specimens.

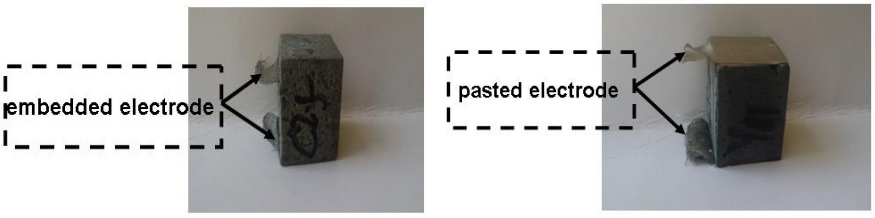

(a)The specimen with embedded electrodes (b)The specimen with pasted electrodes

Fig. 1 - The specimens used in this research.

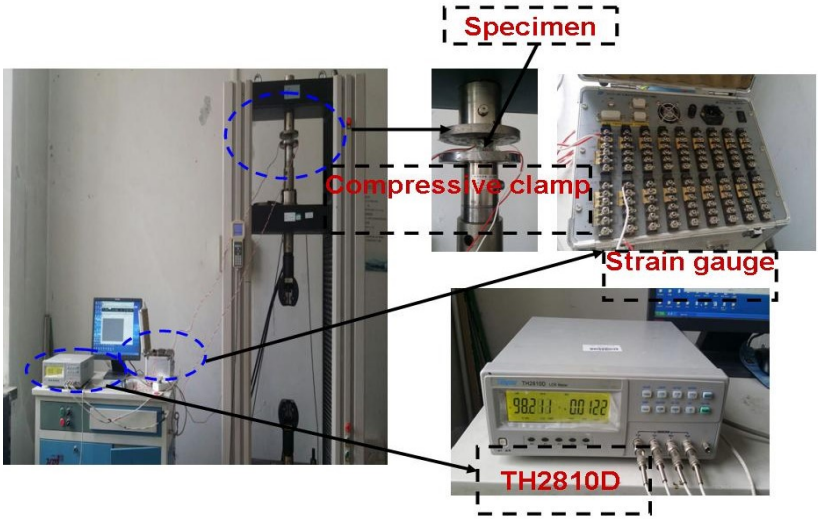

Fig. 2 - The equipment for piezoresistivity measuring.

The piezoresistivity measurement was carried out by using a universal material testing machine with a maximum loading capacity of 100 kN and displacement loading of 0.1mm/min rate as shown in Figure 2. The stress(σ) was applied on the longitudinal direction of the specimen. The σ was increased from 0 MPa to 15MPa during the load process.

A TH2810D LCR digital electric bridge was used to collect electrical signals at the loading process with the testing frequency of 10 kHz. A strain gauge was used to measure the strain of CNFP during the load. The same experimental method and procedure was performed as described in Ref [20]. Three specimens with similar resistivity were tested for each mixture.

The fractional change in electrical resistivity (*FCR*) can be represented as following:

$$FCR = \frac{R - R_0}{R_0} \quad (3)$$

Where R_0 is the initial resistance of the specimen before loading, R is the resistance during the process of loading.

3. Results and discussion

3.1. The influence of AC frequency on resistivity

The average resistivity of CNFP with embedded electrodes or pasted electrodes at different AC frequency is shown in Figure 3. It could be observed that the resistivity decreased sharply with the increasing frequency of AC voltage when CNFs addition was below 2.5vol.%. As the content of CNFs reached 2.5vol.% or higher, the resistivity barely changed with AC frequency.

The value of C_v shows a similar tendency to the mean resistivity value with the various AC frequency, as illustrated in Figure 4. The results indicated that higher AC voltage frequency could reduce the resistivity and improve the stability of resistivity values as the adding dosage of CNFs was less than 2.5vol.%. When the dosages of CNFs achieved 2.5vol.% and hihger, the frequency has no significant influence on the resistivity. This was possibly due to the relatively complete conductive net when the CNF content reached 2.5vol.%. At this CNF content the ionic conduction and electric polarization had little

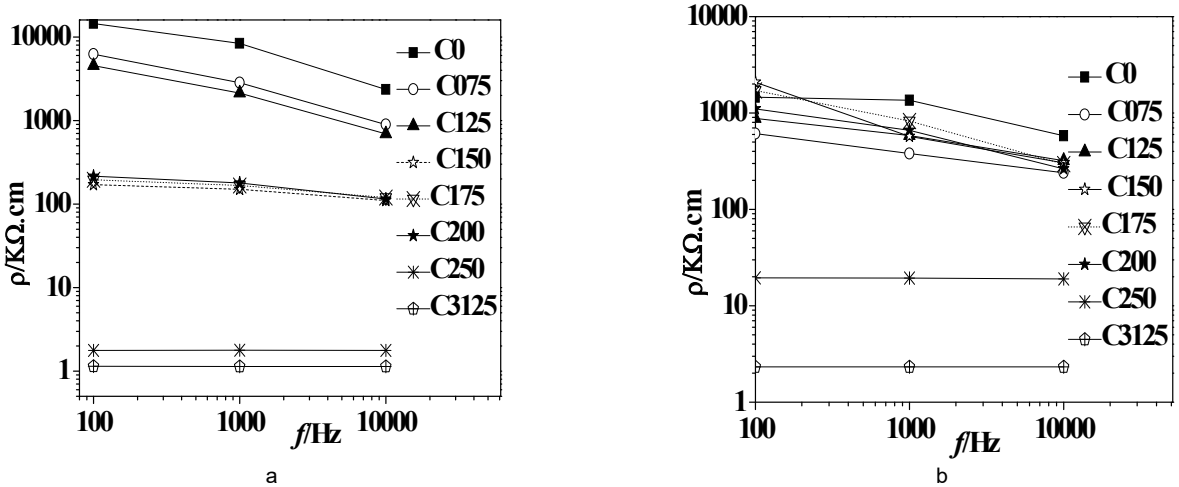

Fig .3 - The average resistivity of CNFP with (a) Embedded electrodes; (b) Pasted electrodes.

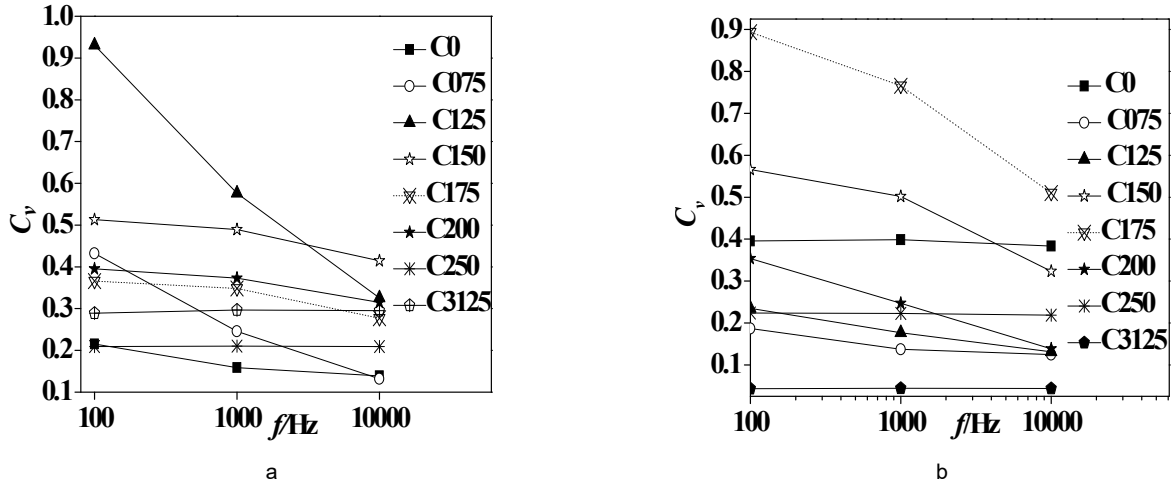

a b

Fig .4 - The C_v of CNFP with (a) Embedded electrodes; (b) Pasted electrodes.

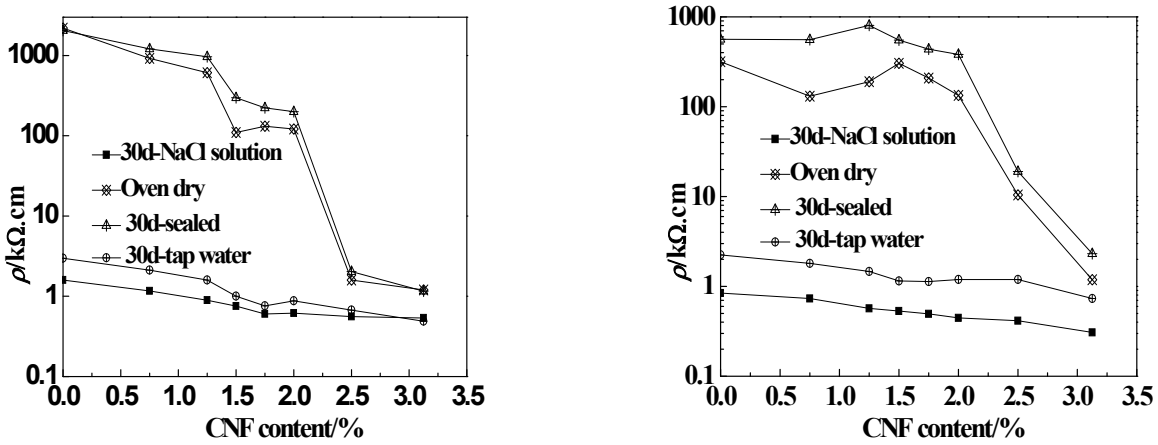

a b

Fig .5 - The average resistivity of CNFP exposed to different conditions for 30 days (a) embedded electrode; (b) pasted electrode..

influence on the electrical properties of the specimen. Therefore, the resistance measured by AC method rarely changes with the testing frequency of AC voltage.

The resistivity and C_v of the CNFP specimens with pasted electrode were higher than CNFP with embedded electrode when the amount of CNFs was less than 3.125 vol.%. While their difference were very little when CNFP contained more than 2.5 vol.% of CNFs. In this case the resistance was determined with each frequency. This phenomenon could be explained by the higher contact resistance between electrodes and specimen for pasted electrode samples. As the content of CNFs was more than 2.5 vol.%, the resistivity of CNFP with pasted electrodes was nearly equal to CNFP with embedded electrodes. This might be due to the reduced contact resistance of CNFP with pasted electrodes.

3.2. The influence of saturation state on resistivity

The resistivity of CNFP decreased dramatically by exposure to water or NaCl solution respectively for 30 days as the CNF content was lower than 2.5vol.%, as shown in Figure 5. The

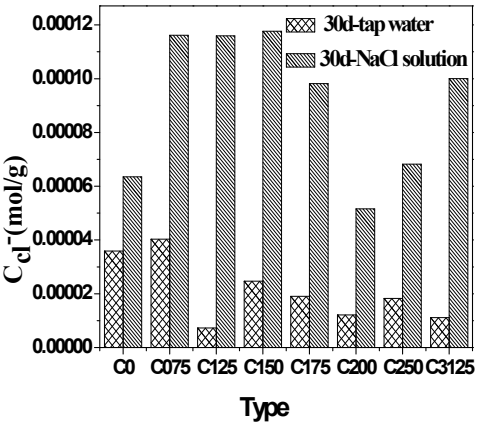

Fig . 6 - Chloride ion concentration in CNFP after different exposure for 30 days.

resistivity of CNFP with CNF content below 2.5vol.% declined more heavily by the immersion in NaCl solution than the immersion in water. This may be attributed to the increase of chloride ions content (seen in Figure 6). However, the water and chloride ions had almost no significant effect on the resistivity of CNFP when the CNFs dosage reached 2.5 vol.%. Similar to the results shown in Fig.3, the resistivity of CNFP with pasted electrodes was higher than

that with embedded electrodes when the CNF content was lower than 3.125 vol.%. As the CNFs content reached 3.125 vol.%, the resistivity of specimens with two types of electrodes were approximately equal.

From the above results and analysis, it could be concluded that the specimen with embedded electrodes had less contact resistance when CNFs content was lower than 3.125 vol.%. However, as the CNF content reached 3.125 vol.%, the resistivity of CNFP with two types of electrodes were almost the same. This is attributed to the integrity and the reduced contact resistance of the specimen with pasted electrodes [14].

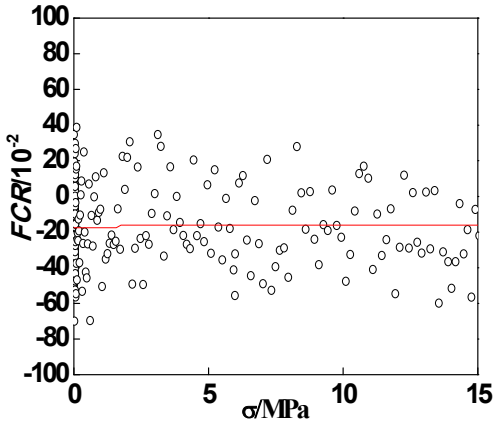

(a) C0-embedded electrode

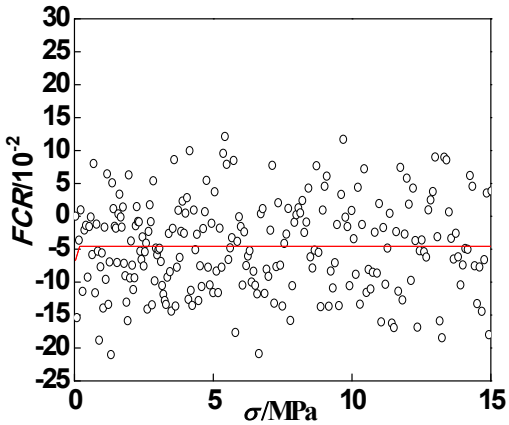

(c) C075-embedded electrode

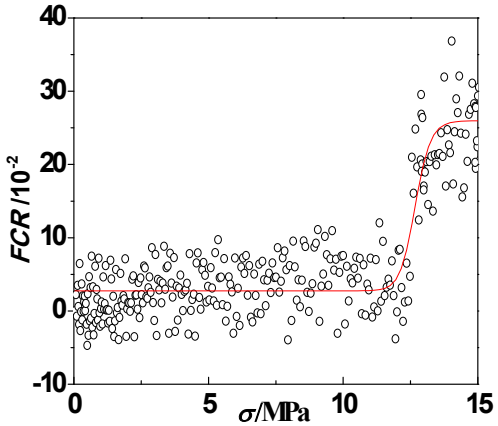

(e) C125-embedded electrode

3.3. The piezoresistivity measurement

The experimental result of piezoresistive performances and the regressed curve between *FCR* and *σ* for every specimen are shown in Fig. 7 and Table 1 respectively. The CNFP presented absent or low sensitivity with CNFs content below 2.5 vol. %. At these dosages, the tunnel current in material could not form and the electrical barrier was not short enough [23]. In this conductive zone, the conductive path is hard to form, even though an external force is applied to the CNFP. As a result, the cement paste performed poor or no sensitivity [16, 24]. The CNFP with pasted electrodes was less sensitive than the embedded electrodes unless the CNF content

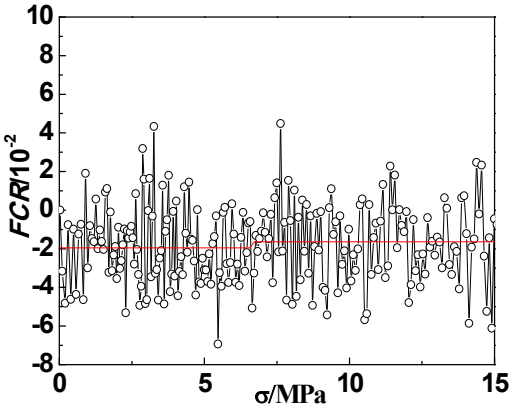

(b) C0-pasted electrode

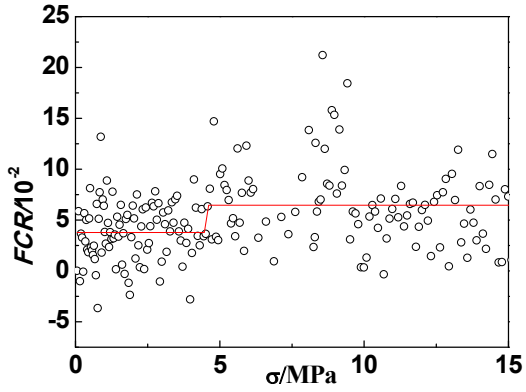

(d) C075-pasted electrode

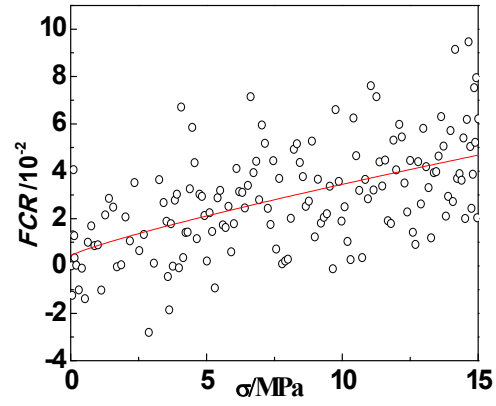

(f) C125-pasted electrode

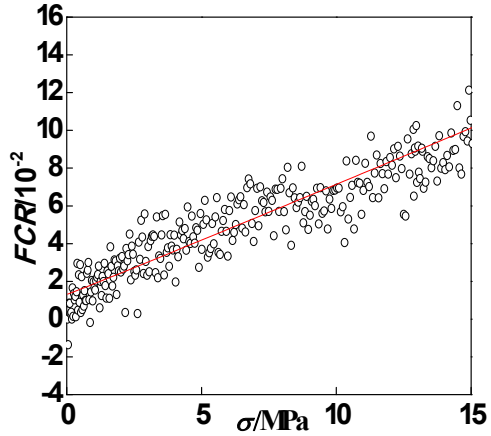

(g) C150-embedded electrode

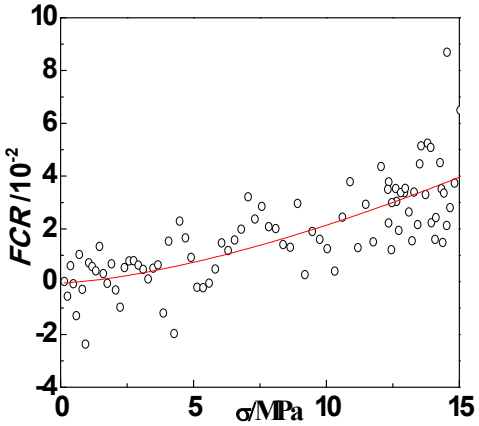

(h) C150-pasted electrode

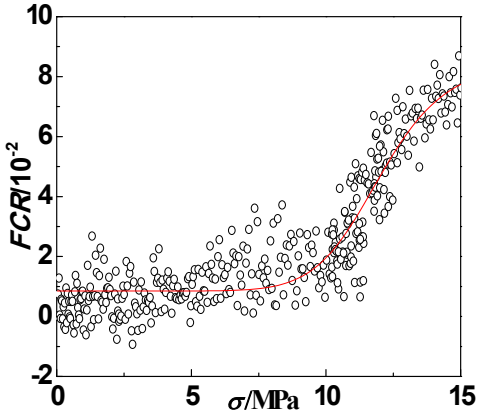

(i) C175-embedded electrode

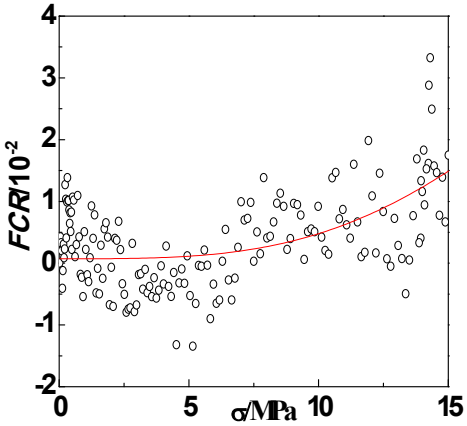

(j) C175-pasted electrode

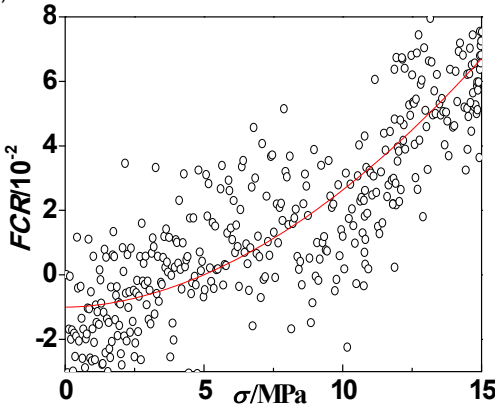

(k) C200-embedded electrode

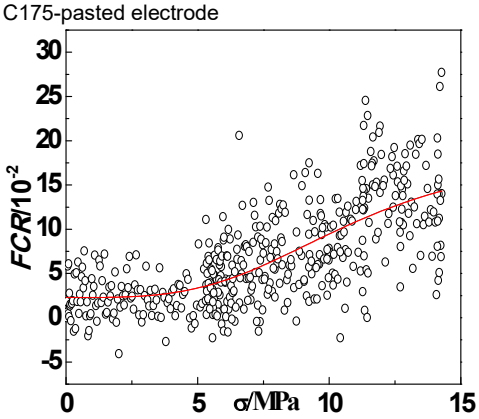

(l) C200-pasted electrode

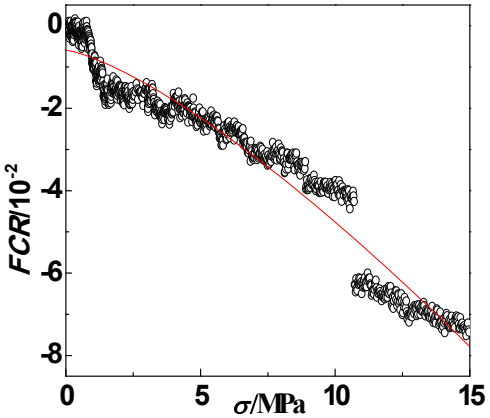

(m) C250-embedded electrode

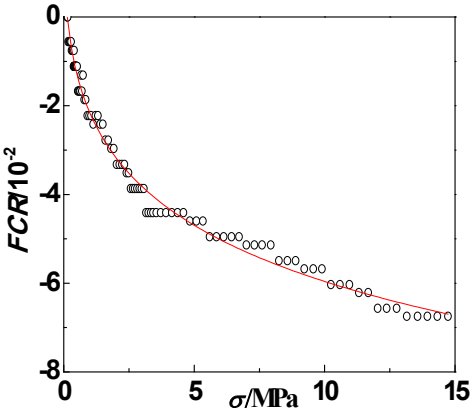

(n) C250-pasted electrode

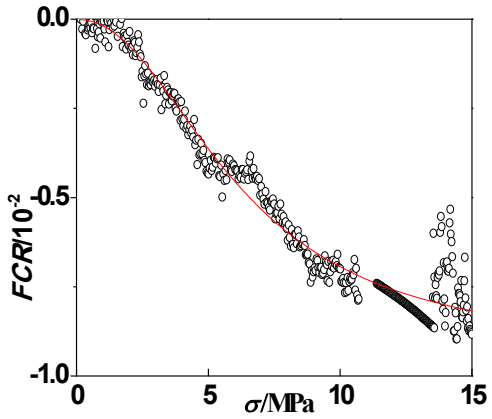

(o) C3125-embedded electrod

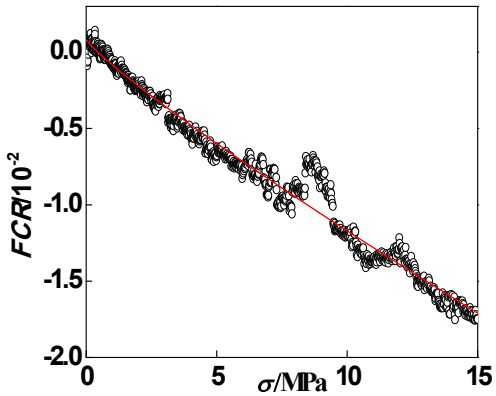

(p) C3125-pasted electrode

Fig. 7 - Piezoresistivity measurement results of CNFP specimens.

Table 1

The fitting results between *FCR* and *σ* for different CNFP.

Equations	Specimen	A_1	A_2	x_0	p	R^2
$FCR = A_2 + \frac{(A_1 - A_2)}{1+(\sigma/x_0)^p}$	C0-embedded	-17.58	-16.14	1.62	2771.05	-0.007
	C075-embedded	-6.68	-4.55	0.13	111.89	-0.011
	C125-embedded	2.75	25.99	12.68	45.08	0.859
	C150-embedded	1.31	627946.2	871927.1	1.02	0.860
	C175-embedded	0.85	8.55	12.02	9.70	0.856
	C200-embedded	-1.00	53986.43	1771.09	1.86	0.71
	C250-embedded	-0.59	-244894	35235.92	1.34	0.95
	C3125-embedded	-9.99E-04	-0.93	6.16	2.18	0.97
	C0-pasted	-1.95	-1.64	6.71	150761.3	-0.0076
	C075-pasted	3.77	6.46	4.57	1128.09	0.11477
	C125-pasted	0.43	35888.53	659004.3	0.85	0.30
	C150-pasted	-0.047	9578.54	2787.10	1.49	0.46
	C175-pasted	0.072	9.82	25.40	3.36	0.432
	C200-pasted	2.28	18.98	10.84	3.45	0.49
	C250-pasted	2.56	-18.19	26.28	0.37	0.99
	C3125-pasted	0.082	-11696.4	314023.1	0.88	0.98

reached 2.5 vol.%. The reason was probably attributed to higher contact resistance of the specimen with pasted electrodes.

As seen in Figure 7, the maximum value of *FCR* was performed by C250 at the peak point. The resistance of CNFP was decided by the following factors including the tunneling distance, contact condition among CNFs and the bonding state between CNFs and matrix. The main factor that affects the resistance of CNFP was the bonding between CNFs and matrix when CNFs content increased from 2.0 vol.% to 2.5 vol.%. It can be seen from the above analysis that the resistance of C250 is easy to change when an external force is applied to the CNFP [25].

However, as the CNFs content reached 3.125 vol.% the parameters of the fitting degree and sensitivity performed worse than the C250 sample, which can be attributed by the contacting conduction between CNFs [24, 26]. In this conductive zone, the change of contact between CNFs and the resistance of CNFs become the dominant conducting factors. The conductive network inside the CNFP stabilizes and becomes hardly changeable under loading. As a result, the CNFP will present poor stable sensing property and low sensitivity [27].

Simmons [28] put forward a universal equation for the conduction of the composite according to the tunneling effect theory. Wang et al. [29, 30] found that the piezoresistive computational model of carbon black composites can be expressed by the following equations.

$$R = R_0(\phi_0 - \phi_c)^t(\phi_0 e^{\frac{1-2\upsilon}{E}\sigma} - \phi_c)^{-t} e^{-\frac{1+2\upsilon}{E}\sigma}$$
$$\frac{\partial FCR}{\partial \sigma} = [-t\phi_0 e^{\frac{1-2\upsilon}{E}\sigma}(\frac{1-2\upsilon}{E})(\phi_0 e^{\frac{1-2\upsilon}{E}\sigma} - \phi_c)^{-1} - \frac{1+2\upsilon}{E}]RR_0^{-1}$$
$$FCR = \int_0^{\sigma}[-t\phi_0 e^{\frac{1-2\upsilon}{E}\sigma}(\frac{1-2\upsilon}{E})(\phi_0 e^{\frac{1-2\upsilon}{E}\sigma} - \phi_c)^{-1} - \frac{1+2\upsilon}{E}]RR_0^{-1}d\sigma$$
$$= -(\phi_0 - \phi_c)^t(\phi_0 e^{\frac{1-2\upsilon}{E}\sigma} - \phi_c)^{-t} e^{-\frac{1+2\upsilon}{E}\sigma}[t\phi_0 \ln(\phi_0 e^{\frac{1-2\upsilon}{E}\sigma} - \phi_c) - \frac{1+2\upsilon}{E}\sigma] \quad (4)$$

Where t is the percolation coefficient of the composite, ϕ_0 is the volume fraction of conductive fillers without load and ϕ_c is the percolation threshold of the conductive fillers, E is the elastic modulus of the specimen, υ is the Poisson ratio of the specimen.

However, the piezoresistive computational model of Wang [30, 31] was obtained when the stress strain state was in the elastic stage. It must be noted that the relationship between *FRC* and σ of self-sensing material could be well defined by a nonlinear curve [1, 2, 8] similar to the findings in this paper. As the above fitting results, the *FCR* of CNFP can be described by:

$$FCR = A_2 + (A_1 - A_2)/(1 + (\sigma/x_0)^p) \quad (5)$$

Where R_0 is the initial resistance of the specimen before load, A_1, A_2, x_0 and p are the constants.

As observed in Figure 7 and Figure 8, CNFP demonstrated poor self-sensing phenomenon as the dosage was less than 2.5vol.% that meant 20 kΩ.cm<ρ_0 (ρ_0 is the initial resistivity). In this condition the CNFP with embedded electrodes had a better fitting degree between *FCR* and σ than that with pasted electrodes. The CNFP with pasted electrodes presented a better fitting degree as the CNF content was more than 2.5vol.%, in other words 0<ρ_0<20kΩ.cm.

Figure 9 shows the axial compressive strength of CNFP. The axial compressive strength of CNFP increased with the volume of CNFs varying from 0 vol.% to 2.0 vol.%. As the content of CNFs reached 2.5 vol.% or higher, the axial compressive strength

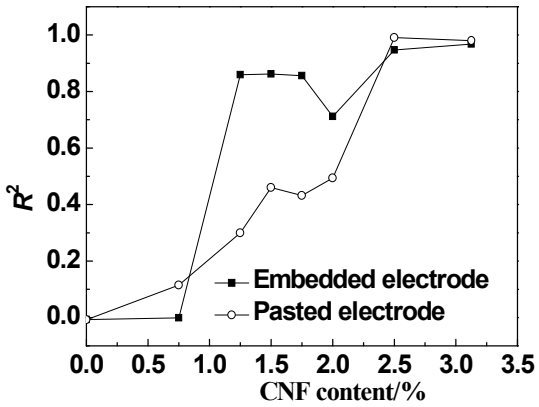

Fig. 8 - R^2 of the fitting equations between electrical resistance variation and stress.

decreased. The axial compressive strength of CNFP with embedded electrode was a little higher probably due to the reinforced effect of stainless steel net. Generally, the axial compressive strength of CNFP specimen was improved by the CNFs.

The stress strain curve of CNFP with different CNFs content is observed in Figure 10. The stress strain curve indicates that as the CNF content increased from 0vol.% to 2.0 vol.%, the CNFs could improve the ductility and axial compressive strength at the same time. However, when the CNF content increased to 2.5 vol.% or hihger, the ductility and axial compressive strength decreased notably, possibly due to the CNFs agglomerating effects in the cement matrix. The ductility of CNFP with embedded electrode presented better, this might be attributed to the stainless steel net.

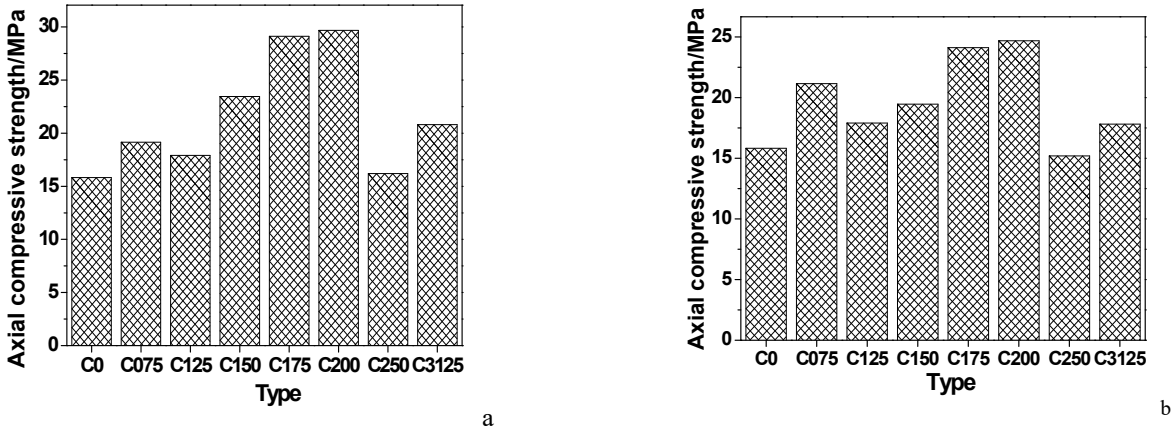

Fig. 9 - The axial compressive strength of CNFP; (a) Embedded electrodes; and (b) Pasted electrodes.

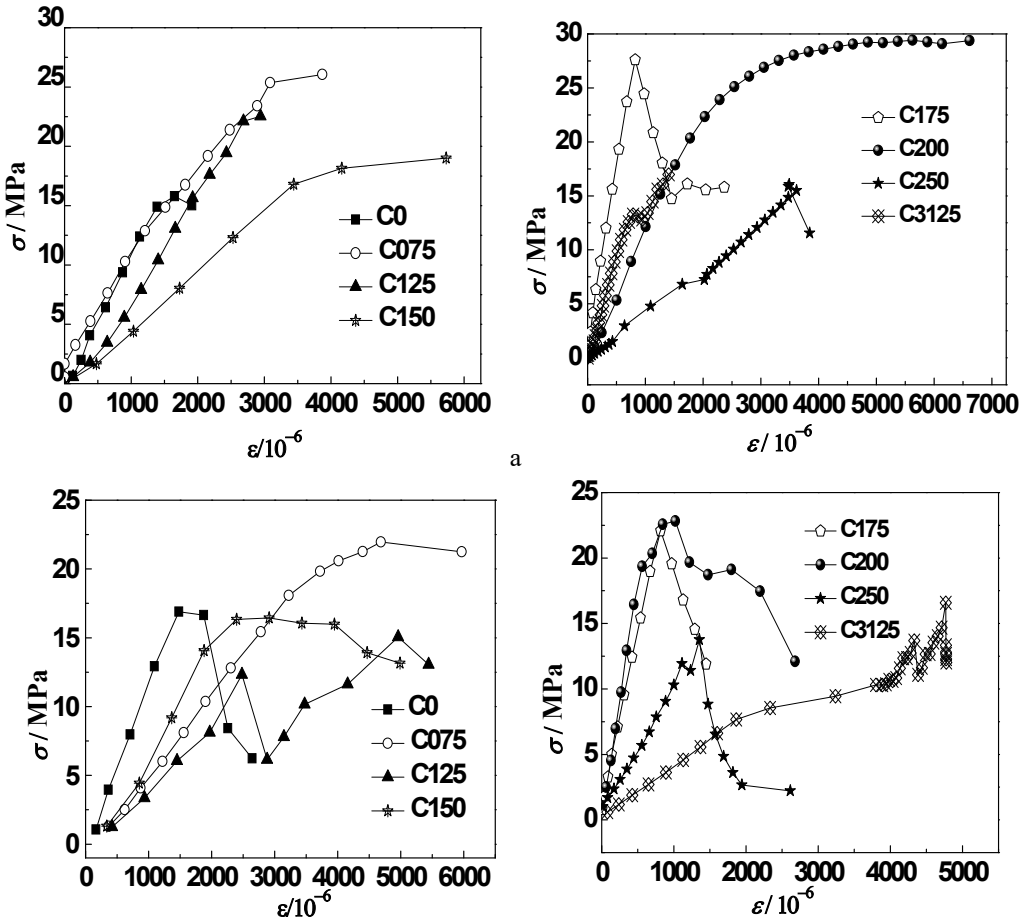

Fig. 10 - The stress-strain curve of CNFP; (a) Embedded electrode; (b) Pasted electrode.

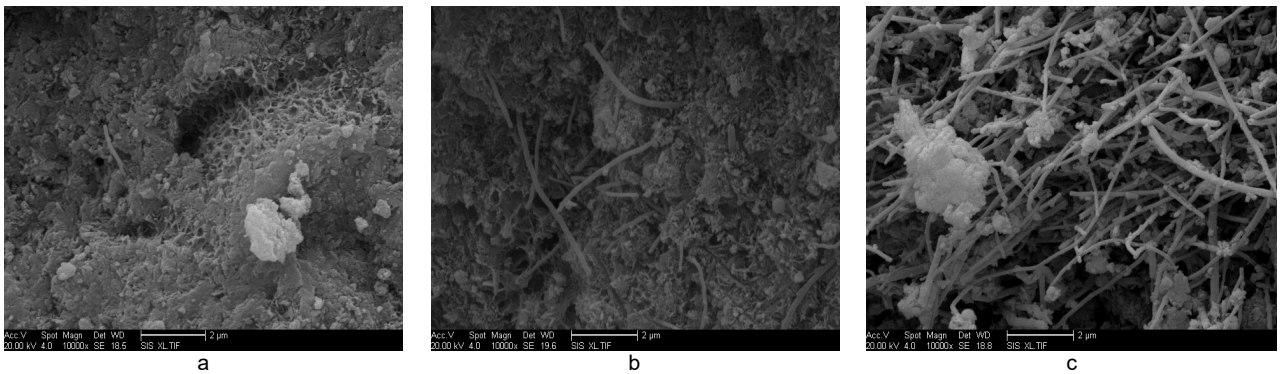

Fig.11 - SEM observation of CNFP. (a) C075; (b) C250; (c) C3125

3.4. Microscopic observation

The scanning electron microscope (SEM) observation of CNFP with three dosages of CNFs is illustrated in Figure 11. Fig.11(a) presents the microstructure of CNFP in insulation zone. In this zone, few CNFs can be found in the CNFP, which means the conductive path is hard to form. Fig.11 (b) shows the microstructure of CNFP in percolation zone. In this conductive zone, fillers form conductive link and start forming conductive path; spacing between adjacent fillers decreases. Fig. 11(c) shows the microstructure of CNFP whose CNFs content is close to the conducting zone. In this conductive zone, the filler concentration is much higher than the percolation threshold and conductive fibers can be approximately regarded as being fully contacted each other.

4. Conclusions

(1) The resistivity of CNFP was decreased by high AC frequency when the CNFs addition was less than 2.5vol.%. The frequency had no significant influence on CNFP resistivity containing 2.5 vol. % or higher dosages of CNFs.

(2) The immersion of water and NaCl solution decreased the resistivity of CNFP significantly

due to the increasing amount of ions in specimen. This influence presented very weak when the CNFs content increased to 2.5vol.% or higher.

(3) The CNFP with embedded electrodes presented better piezoresistive performance when the CNFs addition was less than 2.5vol.%. The result was opposite when the CNFs content reached 2.5 vol.% or hihger. The piezoresistive computational model for CNFP was $FCR=A_2+(A_1-A_2)/(1+(\sigma/x_0)^p)$ in this paper. There was no obvious sensitivity unless the resistivity of CNFP decreased to 20kΩ.cm.

(4) The CNFP specimens with suitable CNFs content resulted in the improved ductility and axial compressive strength.

Acknowledgements

This work was supported by the Program for New Century Excellent Talents in University [NCET-12-0157] and the Natural Science Foundation of Heilongjiang Province –China (E201313).

REFERENCES

1. J. Ou. Some recent advances of intelligent health monitoring systems for civil infrastructures in HIT. Proceedings of SPIE-The International Society. 2005, 5851.
2. Z.P. Szewczyk, P. Hajela. Damage Detection in Structures Based on Feature Sensitive Neural Networks. Journal of Computing in Civil Engineering. 1994, **8**(2), 163.
3. D. Maity, A. Saha. Damage assessment in structure from changes in static parameter using neural networks. Sadhana, 2004, **29**(3), 315.
4. P. C. Aitcin. Cements of yesterday and today: Concrete of tomorrow. Cement and Concrete Research, 2000, **30**(9),1349.
5. P.W. Chen, D.D.L. Chung. Concrete as a new strain/stress sensor. Composites Part B: Engineering. 1996, **27**(1), 11.
6. H. De Backer，W. De Corte，P. Van Bogaert. A case study on strain gauge measurements on large post-tensioned concrete beams of a railway support structure. Or Insight, 2003, **45**(45), 822.
7. H.N. Li，D.S. Li，G.B. Song. Recent applications of fiber optic sensors to health monitoring in civil engineering. Engineering Structures, 2008, **26**(11), 1647.
8. H. Gu. Health monitoring of a concrete structure using piezoceramic materials. Proceedings of SPIE-The International Society, 2005, **57- 65**, 108.
9. S.J. Savage. Engineering aspects of shape memory alloys. International Materials Reviews, 1990, **36**(4), 273-273.
10. H. Inada, Y. Okuhara, H. Kumagai. Experimental study on structural health monitoring of RC columns using self-diagnosis materials. Smart Structures and Materials, 2004, **5391,** 609.
11. O.O.A. Oni, M. Capper, C. Soutis. Monitoring fracture healing with strain gauges: the effect on strain values of strain gauge location on the pin circumference. Injury-international Journal of the Care of the Injured. 1995, **26**(3),181.
12. F. Yu, M. Kahrizi. Characterization of a FBG strain gage array embedded in composite structure. Sensors and Actuators A Physical, 2005, **121**(2), 297.
13. D.D.L. Chung. Strain sensors based on the electrical resistance change accompanying the reversible pull-out of conducting short fibers in a less conducting matrix. Smart Materials and Structures. 1995, **4**(1), 59.
14. B. Han, J. Ou. Embedded piezoresistive cement-based stress/strain sensor. Sensors and Actuators A Physical, 2007, **138**(2), 294.
15. H.K. Kim, I.S. Park, H.K. Lee. Improved piezoresistive sensitivity and stability of CNT/cement mortar composites with low water–binder ratio. Composite Structures, 2014, **116**(1), 713.
16. H. Li, H.G. Xiao, J.P. Ou. Effect of compressive strain on electrical resistivity of carbon black-filled cement-based composites. Cement and Concrete Research. 2006, **28**(9), 824.
17. Konsta-Gdoutos MS, Aza CA. Self sensing carbon nanotube (CNT) and nanofiber (CNF) cementitious composites for real time damage assessment in smart structures. Cement and Concrete Composites. 2014, **53,** 162.
18. F. Reza, G.B. Batson, J.A. Yamamuro. Volume Electrical Resistivity of Carbon Fiber Cement Composites. Aci Materials Journal, 2001, **98**(1), 25.
19. G. Gary, Tibbetts, L. Max, Lake, L. Karla. Strong, Brian P. Rice-A review of the fabrication and properties of vapor-grown carbon nanofiber/polymer composites. Composites Science and Technology. 2007, **67**(7-8), 1709.
20. B. Han, X. Guan, J. Ou. Electrode design, measuring method and data acquisition system of carbon fiber cement paste piezoresistive sensors. Sensors and Actuators A Physical, 2007, **135**(2), 360.
21. GB175-2007, Common Portland cement. *China Standard Press*, 2007(in Chinese).
22. L. Zhou, Y. Cai, H. Zhou. A Concise Course in University Physics. Chemistry Industry Press (2006).
23. P. Sheng，E.K. Sichel，J.I. Gittleman. Fluctuation-induced tunneling conduction in carbon polyvinylchloride composites. Physical Review Letters, 1978, **40**(18), 119- 7-1200.
24. G.Y. Li, P.M. Wang, X. Zhao. Pressure-sensitive properties and mic- rostructure of carbon nanotube reinforced cement composites. Cement and Concrete Composites, 2007, **29**(5), 377.
25. X. Wang, Y Wang, Z. Jin. Electrical conductivity characterization and variation of carbon fiber reinforced cement composite. Journal of Materials Science, 2001, **37**(1), 223.
26. B.G. Han. Properties, Sensors and Structures of Pressure-Sensitive Carbon Fiber Cement Paste, Dissertation for the Doctor Degree in Engineering, Harbin Institute of Technology, China, 2005.
27. P. Xie, P. Gu, J.J. Beaudoin. Electrical percolation phenomena in cement composites containing conductive fibres. Journal of Materials Science, 1996, **31**(15), 4093.
28. J.G. Simmons. Effective tunnel effect between dissimilar electrodes separated by a thin insulating film. Journal of Applied Physics, 1963, **34**(9), 2581.
29. Y. Wang, X. Zhao. Positive and negative pressure sensitivities of carbon fiber-reinforced cement-matrix composites and their mechanism. Acta Materiae Compositae Sinica, 2005, **22**(4),40.
30. P. Wang, T. Ding, X.U. Feng, Y. Qin. Conductivity and piezoresistivity of conductive carbon black filled polymer composite. Journal of Applied Polymer Science, 2010, **116**(4), 2035.
31. S.L. Wang, P. Wang, T.H. Ding. Piezoresistivity of silicone-rubber/carbon black composites excited by AC electrical field.Journal of Applied Polymer Science, 2009 , **113** (1) :337-341.

****